



Modification of polysulfone ultrafiltration membrane by sequential deposition of cross-linked poly(vinyl alcohol) (PVA) and sodium carboxymethyl cellulose (CMCNa) for nanofiltration

Yuhao Zhang^a, Chuang Yu^a, Zhenhua Lü^{a,b}, Sanchuan Yu^{a,*}

^aDepartment of Chemistry, Zhejiang Sci-Tech University, Hangzhou 310018, China, Tel./Fax: +86 571 86843217; emails: zyh130913@163.com (Y. Zhang), yu199412boy@163.com (C. Yu), yuschn@163.com (S. Yu)

^bCentre for Membrane Technology, Hangzhou Tianchuang Environmental Technology Co. Ltd, Hangzhou 311121, China, Tel./Fax: +86 571 88513915; email: lvxf136@139.com

Received 9 April 2015; Accepted 22 August 2015

ABSTRACT

This study focused on the modification of flat-sheet polysulfone ultrafiltration membranes for nanofiltration (NF) through sequential deposition of poly(vinyl alcohol) (PVA) and sodium carboxymethyl cellulose (CMCNa) with glutaraldehyde cross-linking after each deposition. The contents of PVA and CMCNa in the coating solutions were varied to optimize the membrane performance and the modified membranes were characterized in terms of surface and permeation properties. It was found that the membrane surface became denser, more hydrophilic, and negatively charged at neutral pH after modification and the modified membrane possessed the NF separation characteristic. Under 5.0 bar, the optimized modified membrane exhibited a high-pure water flux of 89.5 l/m² h and rejections of 37.8 and 93.8% to 500 mg/l NaCl and Na₂SO₄ aqueous solution, respectively. The modified membrane could also efficiently remove anionic dyes from aqueous solution, showing retentions of 99.7 and 99.5% to methyl blue and congo red, respectively, under neutral pH and 5.0 bar. Additionally, the modified membrane possessed good chlorine stability, and acid and alkaline resistances. The technique developed is potentially applicable for the fabrication of high-flux negatively charged NF membranes for partial desalination and anionic dye removal.

Keywords: Nanofiltration; Thin-film composite membrane; Membrane modification; Poly(vinyl alcohol) (PVA); Sodium carboxymethyl cellulose (CMCNa); Dye removal

1. Introduction

Nanofiltration (NF) membrane has been widely used in the fields of water and wastewater treatment, partial desalination, and industrial fluids separation for its key distinguishing characteristics of low

rejection to monovalent ions, high rejection to multivalent ions, and higher water permeability compared to reverse osmosis (RO) membranes [1–7]. However, the most commercially available polyamide composite NF membranes are faced with two major obstacles of low chemical stability and poor chlorine tolerance. Therefore, it is still of great interest to investigate the novel NF membranes with high

*Corresponding author.

chemical stability, good chlorine tolerance as well as high separation performance [8].

Poly(vinyl alcohol) (PVA), as a water-soluble biodegradable polymer with inherent hydrophilicity, good film-forming property, and excellent chemical stability, has been adopted to fabricate membranes having the characteristics of high chemical stability, good chlorine tolerance, and low fouling [9] for a number of separation processes including microfiltration [10], ultrafiltration [11], RO [12], and pervaporation [13]. It has also been exploited as the barrier layer for the preparation of composite NF membranes through solution coating followed by chemical cross-linking [14–18]. However, most of the PVA composite NF membranes exhibit relatively low water permeability and poor solute selectivity, since the separation of the PVA NF membrane with neutral selective skin layer depends solely on size exclusion [19].

Compared with the neutral NF membrane, charged NF membranes are preferable for better membrane performance, since the separation of charged membrane relies not only on the sieving effect, but also on the Donnan effect [20]. Additionally, the hydrophilic surface of the charged membrane also benefits fouling reduction since it can increase the membrane wettability and thus provide a better cleaning efficiency [21]. Thus, as one of the best candidates that can provide these characteristics to membrane surface, polyelectrolyte offers a new solution to improve the NF membrane's performance. Polyelectrolytes such as quaternary ammonium cellulose ether [22], sodium carboxymethyl cellulose (CMCNa) [23], polystyrene sulfonate [24], polyallylamine hydrochloride [25], and poly(diallyl dimethyl ammonium chloride) [26] have been investigated to fabricate the composite NF membranes through methods such as static deposition, dynamic deposition, single-layer coating, layer-by-layer coating, and so forth. However, the coating of polyelectrolyte is quite influenced by the material and molecular weight cut-off of the support and most of the prepared polyelectrolyte-based membranes have the trade-off problem between permeability and selectivity [27].

Accordingly, in this study, unlike the method of incorporation polyelectrolyte into the PVA matrix to prepare composite NF membranes [28–33], the approach of sequential deposition of PVA and CMCNa on polysulfone ultrafiltration support membrane was adopted to prepare the composite NF membrane. Glutaraldehyde (GA) cross-linking was performed after each deposition to improve the stability and enhance the size exclusion effect of the deposited active layers. The coating of PVA

improved the effectiveness of the CMCNa coating. The concentrations of PVA and CMCNa in the coating solutions were optimized to achieve high water permeability and solute selectivity. The physicochemical properties of the resulting modified membranes were characterized through Fourier transform infrared spectroscopy (ATR-FTIR) in attenuated total reflection mode, scanning electron microscopy (SEM), and measurements of surface zeta potential and water contact angle. The membrane permeation properties including water permeability, molecular weight cut-off, and rejections to different electrolytes and organic dyes were characterized via cross-flow permeation tests.

2. Materials and methods

2.1. Materials and reagents

The flat-sheet polysulfone (PSf) ultrafiltration support membrane with a molecular weight cut-off (MWCO) of around 90,000 Da and a pure water permeability of approximately 110 l/m² h bar was provided by Hangzhou Tianchuang Environmental Technology Co. Ltd, China. CMCNa (degree of substitution: 0.65) with an intrinsic viscosity of 850.8 ml/g in 0.01 M sodium chloride (NaCl) aqueous solution at 25.0°C was purchased from Sinopharm Chemical Reagent Co. Ltd, China. Poly(vinyl-alcohol) (PVA, hydrolysis degree = 98%, Mw = 72,000 g/mol) was purchased from Sigma–Aldrich. Cross-linking agent GA was obtained from Tianjin Kemiou Chemical Reagent Co. Ltd, China.

Inorganic salts such as NaCl, MgCl₂, Na₂SO₄, and MgSO₄ of analytical grade were used as the model electrolytes to determine the permeation characteristics of the resultant membrane. Polyethylene glycol (PEG) fractions with molecular weights of 600, 1,000, 2,000, 4,000, and 6,000 Da purchased from Sigma–Aldrich were used as the model neutral solutes to estimate the MWCO of the obtained membrane.

Organic anionic dyes such as congo red (Fisher Scientific, Hong Kong), methyl blue (Shanghai Specimen and Model, China), and sunset yellow (Aladdin) were used as model solutes to investigate the dye removal performance of the obtained membrane. The molecular structures of the dyes are shown schematically in Fig. 1.

Deionized water with a resistivity of 18.0 MΩ was used to prepare the aqueous solutions for membrane modification and performance evaluation as well as to rinse the membrane samples. All other chemicals involved were all of analytical grade and used without further purification.

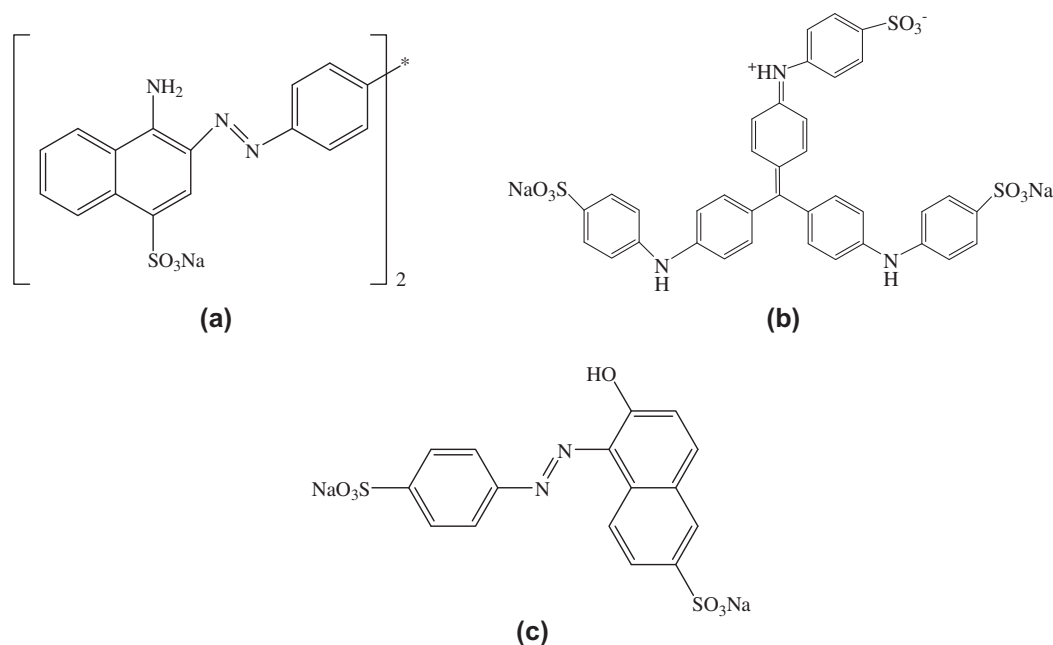


Fig. 1. Molecular structures of the organic dyes used in the experiments: (a) Congo red, (b) Methyl blue, and (c) Sunset yellow.

2.2. Modification of PSf ultrafiltration support membrane

Modification of polysulfone ultrafiltration support membrane was conducted by employing a four-step process: (1) to begin with, an aqueous coating solution containing certain content of PVA ranging from 0.025 to 0.075 wt% was firstly poured onto the surface of the porous PSf support membrane that has been fixed in a polyfluortetraethylene (PTFE) frame. After a residence time of 30 min, the coating solution was drained off and the coated support membrane was air-dried at room temperature until no liquids remained; (2) then, the surface of the precoated support membrane was contacted with an aqueous solution containing 1.0 wt% GA and 0.5 wt% H_2SO_4 for 1.0 min, and the membrane sample was air-dried for 30.0 min, and cured under 60.0°C for 10 min before being thoroughly washed with deionized water; (3) after that, the surface of the PVA-coated membrane was further coated with the second aqueous solution containing certain amount of CMCNa, ranging from 0.05 to 0.15 wt%, by repeating step 1; (4) finally, the membrane sample was treated with GA aqueous solution again by repeating step 2 and the obtained membrane was washed thoroughly with deionized water and stored wetly.

2.3. Membrane acid and alkaline treatments

Membrane acid and alkaline treatments were carried out using 0.5-M sulfuric acid and sodium

hydroxide aqueous solution, respectively, through soaking tests performed in Pyrex glass bottles covered with PTFE caps. All the membrane samples were immersed in acidic or alkaline aqueous solution for 36.0 h at 25.0°C and then rinsed thoroughly with deionized water and stored wetly for further experiments.

2.4. Membrane chlorine exposure experiments

Membrane chlorine exposure experiments were carried out using commercial sodium hypochlorite aqueous solution (NaClO , effective chlorine content: 10 wt%) through soaking tests performed in Pyrex glass bottles covered with PTFE caps. In the soaking tests, membrane samples were exposed to 2000-mg/l sodium hypochlorite aqueous solution at pH 9.0 and 25.0°C for 15.0 h. The chlorine treated membrane samples were thoroughly rinsed with deionized water and stored wetly until performance evaluation.

2.5. Membrane characterization

Membrane surface chemical composition was analyzed by attenuated total reflectance ATR-FTIR using a Nicolet Aratar 370 FTIR spectrometer with a ZnSe crystal as the internal reflection element with an angle of incidence 45° . Membrane surface morphological structure was investigated through SEM with a field

emission scanning electron microscopy (FE-SEM) (Hitachi S-4800, Japan).

Membrane surface hydrophilicity was studied through contact angle measurements by employing a DSA10-MK2 contact angle analyzer (KRÜSS GmbH, Germany). The sessile drop method was used to measure the contact angle of deionized water (about 0.4 μl) on the dried membrane surface at 25.0°C. At least, 10 measurements on different locations of the membrane sample were performed and averaged to obtain the contact angle of the measured membrane sample.

Membrane surface charge was evaluated through measuring the surface-streaming potential employing an electrokinetic analyzer (EKA, Anton Paar GmbH, Austria) with 0.001-mol/l KCl aqueous solutions at 25.0 \pm 1.0°C and pH ranging from 3.0 to 9.0. Surface zeta potentials were calculated from the measured streaming potentials according to the Helmholtz–Smoluchowski equation [34]. The data presented were average values from three samples of each membrane type.

2.6. Cross-flow permeation tests

Cross-flow filtration tests were carried out employing a lab-scale filtration set-up as described in our previous study [35]. Each permeation cell of the filtration set-up has an effective membrane area of 19.0 cm². All the permeation tests were conducted at the constant temperature of 25.0°C, transmembrane pressure of 5.0 bar, and feed pH of 7.0 \pm 0.2 in a total recirculation model, under which the retentate stream was circulated back to the feed tank while the permeate stream was collected for measurements of volume and solute content if necessary and then returned to the feed tank to maintain a constant feed concentration.

All the membrane coupons loaded in the filtration cells were pressurized under 10.0 bar with deionized water for 2 h before permeation tests to ensure stable flux. The pure water flux of the tested membrane was evaluated with deionized water, while the water flux and solute rejection performance were measured with aqueous solution containing model solute of NaCl, MgCl₂, Na₂SO₄, MgSO₄, PEG fraction, or organic dye. The concentrations of PEG, organic dye, and inorganic salt in the feed aqueous solutions were 50, 100, and 500 mg/l, respectively.

A 60 d long-term permeation test was also conducted with 500-mg/l Na₂SO₄ aqueous solution under the circulation model and operating pressure of 5.0 bar to investigate the durability and performance

stability of the obtained NF membrane. Periodical measurements were carried out to check the permeability and rejection of the tested membrane.

2.7. Analytical methods and measurements

Water flux was determined by measuring the permeate water volume collected over a certain period in terms of liter per square meter per hour (l/m² h) and using the following equation:

$$J = \frac{V}{A \times \Delta t} \quad (1)$$

where J is the volumetric permeate water flux, A is the effective area of the membrane for permeation, and V is the volume of permeation over a time interval Δt .

The observed solute rejection (R_s) was calculated using the following equation:

$$R_s (\%) = \frac{C_f - C_p}{C_f} \times 100 \quad (2)$$

in which C_f and C_p are the solute concentrations in feed and permeate streams, respectively.

PEG concentration was determined using a spectrometric titration at 535 nm after iodine complexation [36]. Dye concentration was measured using an ultraviolet–visible spectrophotometer (UV759, Shanghai, China) at the maximal absorption wavelength of each organic dye. Salt concentration was obtained through measuring the conductivity of the aqueous solution using a conductivity meter (DDSJ-308A, Cany Precision Instruments, China) and comparing the calibration plot drawn between salt concentration and conductivity.

3. Results and discussion

3.1. Modification of PSf ultrafiltration support membrane

In this study, the modification of flat-sheet PSf ultrafiltration support membrane for NF was carried out through sequential deposition of PVA and CMCNa, with GA cross-linking after each deposition. The reactions of GA with PVA and CMCNa are schematically shown in Fig. 2.

The performance of the modified membrane was optimized by varying the concentrations of PVA and CMCNa in the coating solutions. It is obvious from Table 1 that the modified membrane has a good solute separation capability and the performance of the

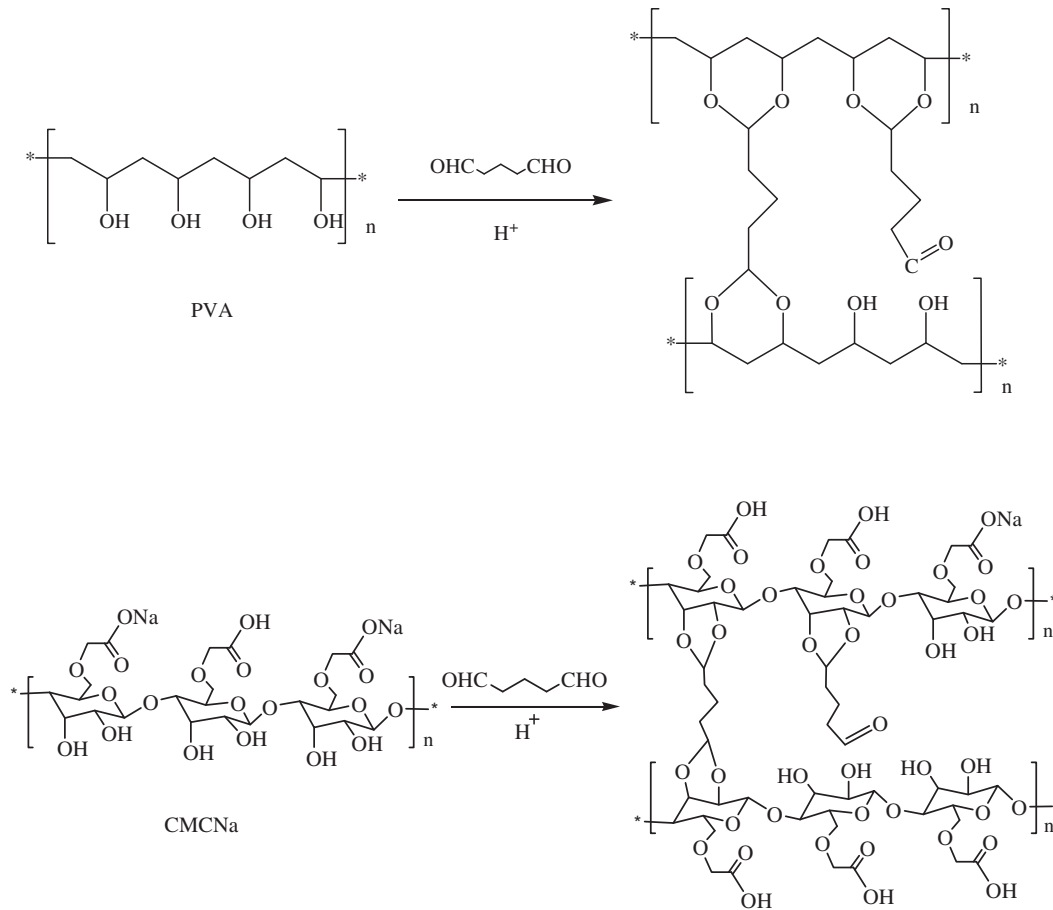


Fig. 2. Schematic diagrams for the reactions of GA with PVA and CMCNa, respectively.

Table 1
Effects of PVA and CMCNa contents on membrane performance

Membrane	PVA content (wt%)	CMCNa content (wt%)	Pure water Flux ^a (l/m ² h)	Rejection to Na ₂ SO ₄ ^b (%)	Rejection to NaCl ^b (%)
NF1	0.025	0.05	105.2 ± 2.5	73.6 ± 0.6	22.5 ± 0.6
NF2	0.05	0.05	95.6 ± 1.6	85.6 ± 0.5	30.7 ± 0.7
NF3	0.075	0.05	74.6 ± 0.6	93.8 ± 0.7	38.0 ± 0.8
NF4	0.05	0.10	89.5 ± 2.0	93.6 ± 0.5	37.6 ± 0.6
NF5	0.05	0.15	66.5 ± 1.5	88.5 ± 0.6	35.2 ± 0.7

^aTested with deionized water under 5.0 bar and 25.0 °C.

^bTested with 500-mg/l salt aqueous solution under 5.0 bar, 25.0 °C, and pH 7.0.

resulting membrane can be modulated through varying the PVA and/or CMCNa contents. With an increase in the PVA content from 0.025 to 0.075 wt% at a fixed CMCNa concentration of 0.05 wt%, the pure water flux of the resultant membrane declines appreciably from 105.2 l/m² h of membrane NF1 to 74.6 l/m² h of membrane NF3, while the rejections to Na₂SO₄

and NaCl ascend from 73.6 to 93.8% and 22.5 to 38.0%, respectively. On the other hand, as the CMCNa content increases from 0.05 to 0.15 wt% at a fixed PVA content of 0.05 wt%, the pure water flux declines sharply from 95.6 l/m² h of membrane NF2 to 66.5 l/m² h of membrane NF5, while the rejections to Na₂SO₄ and NaCl achieve their maximum values at the CMCNa

content of 0.10 wt% (membrane NF4). Higher contents of PVA and/or CMCNa usually result in a denser and thicker skin layer and thereby a lower membrane flux and a higher salt rejection. However, the further decrease in water flux at CMCNa content of 0.15 wt% (membrane NF5) will lead to an overall decline in salt rejection as a result of the concentration buildup in the permeate stream [37].

Considering both water permeability and solute selectivity of the obtained membrane, the relative optimal contents for the PVA and CMCNa coating solutions are 0.05 and 0.10 wt%, respectively. Accordingly, laboratory scale trials were conducted to investigate the repeatability of the membrane modification. The results shown in Table 2 clearly demonstrate that the modification process developed in this study has good repeatability and the obtained modified membrane exhibits a good NF performance, showing average trial-to-trial flux of 89.5 l/m² h to pure water and rejections of 37.8 and 93.8% to 500-mg/l NaCl and Na₂SO₄ aqueous solution, respectively, under 5.0 bar.

3.2. Membrane physicochemical properties

Membrane surface chemical structure was characterized by ATR-FTIR. Fig. 3 presents the spectra of the PSf support membrane, modified membrane with a single cross-linked layer of PVA (PVA/PSf), and modified membrane with cross-linked layers of PVA and CMCNa (CMCNa/PVA/PSf) (trial no. 1). Compared with the spectrum of the PSf support membrane (Fig. 3(a)), the new peaks presented in the spectra of the modified membranes clearly illustrate the presences of PVA, CMCNa, and GA on the surface of the modified membrane. The broad absorption peak at 3,300–3,600 cm⁻¹ of spectrum b is ascribed to the stretching vibration of OH groups of PVA chains [38] and its enhancement in spectrum c is due to the OH groups from CMCNa molecules [39]. The peak at about 1,720 cm⁻¹ (spectra b and c) is attributed to the

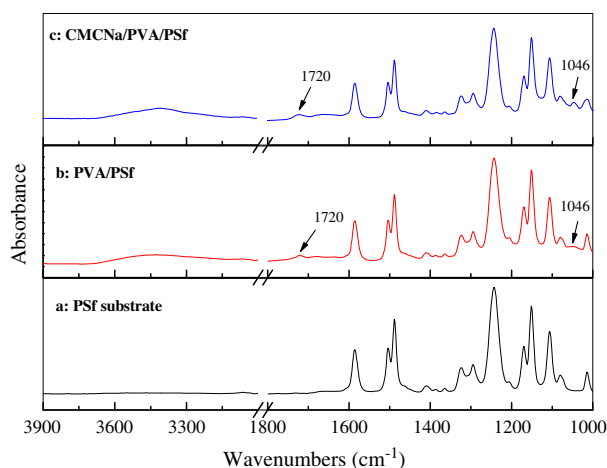


Fig. 3. ATR-FTIR spectra of PSf substrate (a), PVA/PSf modified membrane (b), and CMCNa/PVA/PSf-modified membrane (trial no. 1) (c).

stretching vibration of C=O from the unreacted aldehyde group of GA molecule. Furthermore, the relative weak peak at about 1,046 cm⁻¹ of spectrum b is ascribed to the stretching vibration of C–O–C bonds resulted from the reaction of PVA and GA and its significant enhancement in spectrum c is due to both of the C–O–C bonds from CMCNa chains and the formation of C–O–C bonds through the reaction of CMCNa and GA [39].

Membrane morphological structure was characterized by FESEM and the surface and cross-sectional SEM images of the obtained CMCNa/PVA/PSf composite membrane (trial no. 2) are shown in Fig. 4, which also presents the surface and cross-sectional SEM images of the corresponding PVA/PSf composite membrane and the surface SEM image of the PSf substrate. It can be seen from the figure that both the CMCNa/PVA/PSf and PVA/PSf membranes exhibit a composite structure with a relatively dense skin layer laminated on the surface of the porous PSf support.

Table 2

Pure water fluxes and rejections to Na₂SO₄ and NaCl of the lab-scale modified membranes

Trial no.	Pure water flux ^a (l/m ² h)	Rejection to Na ₂ SO ₄ ^b (%)	Rejection to NaCl ^b (%)
1	90.5	93.4	37.3
2	88.0	94.3	38.5
3	91.5	93.0	36.7
4	89.8	94.0	38.2
5	87.5	94.5	38.6
Average	89.5 ± 1.7	93.8 ± 0.6	37.8 ± 0.8

^aTested with deionized water under 5.0 bar and 25.0°C.

^bTested with 500-mg/l salt aqueous solution under 5.0 bar, 25.0°C, and pH 7.0.

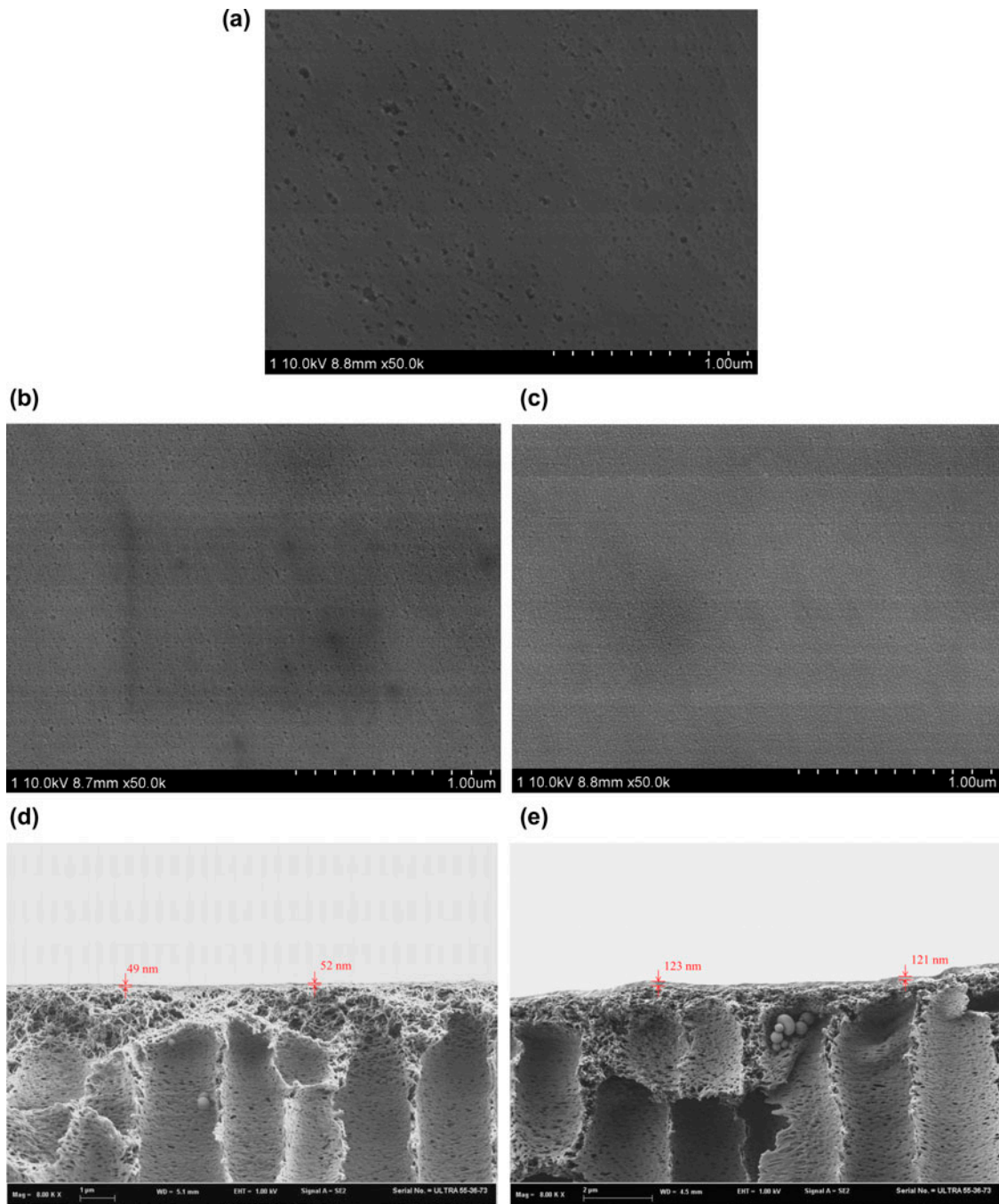


Fig. 4. FESEM images of the surfaces of PSf substrate (a), PVA/PSf composite membrane (b), CMCNa/PVA/PSf composite membrane (trial no. 2) (c), cross sections of PVA/PSf composite membrane (d), and CMCNa/PVA/PSf composite membrane (trial no. 2) (e).

The thickness of the skin layer increases from about 50 nm of the PVA/PSf membrane (Fig. 4(d)) to about 120 nm of the CMCNa/PVA/PSf membrane (Fig. 4(e)).

Membrane surface hydrophilicity was studied through measuring the contact angle between the

membrane surface and the air–water interface and the measured contact angle values are presented in Table 3. The deposition of PVA results in a significant decrease in surface contact angle and the following deposition of cross-linked CMCNa leads to a further decline of surface contact angle, indicating the

Table 3
Surface water contact angle values tested with deionized water at 25.0°C

Membrane	Surface water contact angle (°)
PSf support membrane	83.8 ± 1.5
PVA/PSf composite membrane	69.9 ± 1.3
CMCNa/PVA/PSf composite membrane (trial no. 1)	53.5 ± 1.0

formation of a hydrophilic skin layer on the hydrophobic surface of PSf support membrane.

Membrane surface charge was studied through measuring the surface streaming potential and the measured surface zeta potentials under different pHs are presented in Fig. 5. It is clearly illustrated that all the surfaces of the three tested membranes are negatively charged within the testing pH scope of 3.0–9.0, and the membrane CMCNa/PVA/PSf possesses the highest negative charge under each pH. The surface zeta potential of the obtained CMCNa/PVA/PSf composite membrane (trial no. 1) is about -55 mV under neutral pH.

3.3. Permeation properties

The permeation properties of the obtained modified membrane were investigated in terms of MWCO, rejections to different salts, retentions to anionic organic dyes, and long-term performance.

Membrane MWCO was determined through cross-flow permeation tests using five PEG fractions as neutral model solutes. The MWCO value is taken by

the molecular weight of PEG molecule that is rejected by the membrane to 90% [40]. From the retention curves illustrated in Fig. 6, one can find that the optimized composite membrane obtained through sequential deposition of PVA followed by CMCNa has a MWCO of around 1,400 Da.

Membrane salt rejection characteristic was investigated using four typical salts of $MgCl_2$, NaCl, $MgSO_4$, and Na_2SO_4 through cross-flow permeation tests and the results are presented in Fig. 7. The desired obtained composite membrane exhibits a salt rejection order of $MgCl_2$ (22.8%) < NaCl (38.1%) < $MgSO_4$ (90.2%) < Na_2SO_4 (94.2%), showing a typical salt rejection characteristic of negatively charged polymeric NF membranes. Under neutral pH, the negatively charged membrane surface rejects preferably the anions of higher valence and thus, the rejections to Na_2SO_4 and $MgSO_4$ are higher than those to NaCl and $MgCl_2$. On the other hand, the stronger affinity between the cations of higher valence and membrane surface is the reason for the lower rejections of $MgSO_4$ and $MgCl_2$ compared with Na_2SO_4 and NaCl, respectively [41].

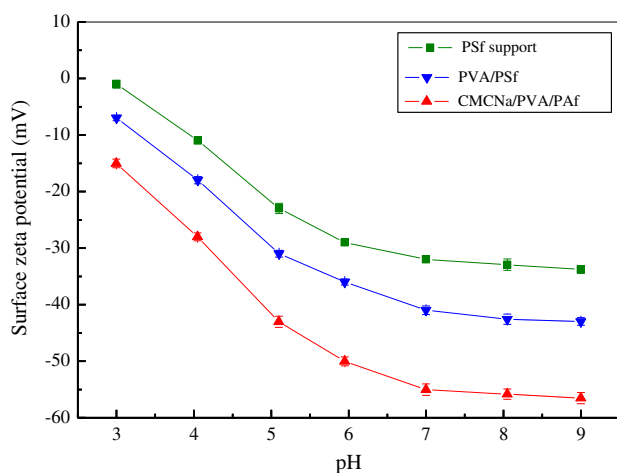


Fig. 5. Surface zeta potential as a function of pH for the PSf support membrane (■), PVA/PSf composite membrane (▼), and CMCNa/PVA/PSf composite membrane (trial no. 1) (▲) tested with 0.001 mol/l KCl aqueous solution and 25.0°C.

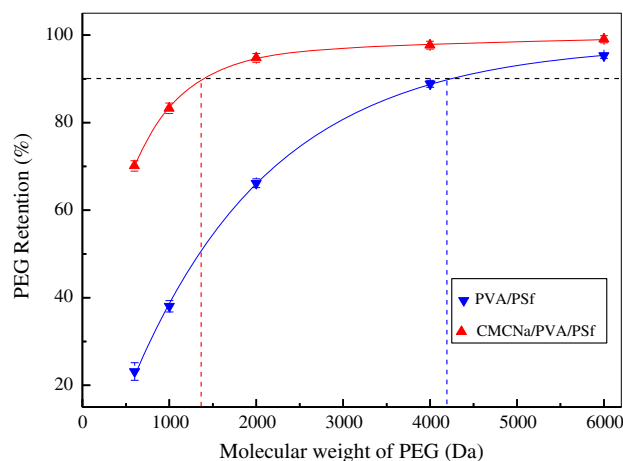


Fig. 6. PEG retention curves of PVA/PSf (▼) and CMCNa/PVA/PSf (trial no. 2) (▲) composite membranes tested with 50-mg/l PEG aqueous solution at 5.0 bar and 25.0°C.

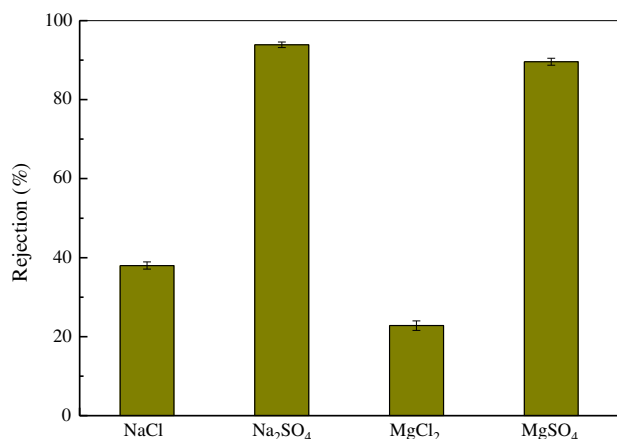


Fig. 7. Rejections to different salts of the CMCNa/PVA/PSf composite membrane (trial no. 4) tested with 500 mg/l salt aqueous solution under 5.0 bar, 25.0°C and pH 7.0.

The dye removal performance of the obtained membrane was also investigated through the cross-flow permeation tests. The time-dependent water fluxes of the tested modified membrane (trial no. 3) to different anionic dye aqueous solutions are illustrated in Fig. 8 and the steady-state dye removal and water flux to each dye aqueous solution are listed in Table 4. The obtained modified membrane can effectively remove the anionic organic dyes from aqueous solution. The removals of methyl blue and congo red are much higher than that of sunset yellow. Dyes with more negative charge and/or higher molecular weight are more efficiently rejected by the membrane for the stronger effects of steric hindrance and electrostatic repulsion [42]. Additionally, the equilibrium flux decline ratios are only 10.4, 13.6, and 16.8% to sunset yellow, methyl blue, and congo red aqueous solutions, respectively. The relatively low flux decline is due to the electrostatic repulsion between the membrane surface and dye molecules which mitigates the adsorption of dye molecules on membrane surface and thereby lighting membrane fouling [43].

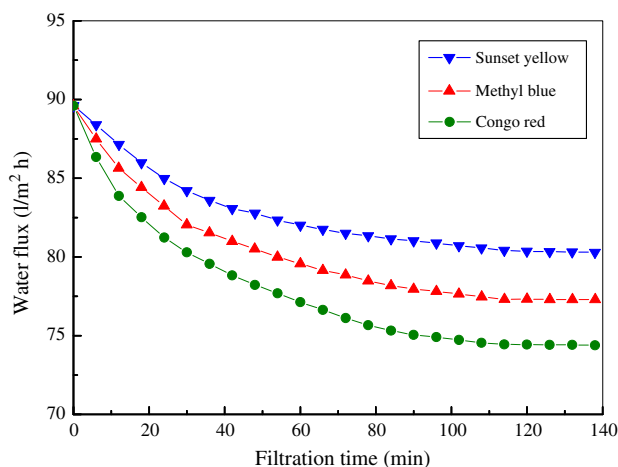


Fig. 8. Time-dependant water fluxes of the CMCNa/PVA/PSf composite membrane (trial no. 3) filtrated with aqueous solution containing different dyes: sunset yellow (▲), methyl blue (▼), and congo red (●). Test conditions: 50-mg/l dye concentration, 5.0 bar, pH 7.0, and 25.0°C.

Fig. 9 illustrates the changes of the water flux and salt rejection of the obtained modified membrane (trial no. 3) during a 60 d continuous filtration of 500-mg/l Na₂SO₄ aqueous solution under 5.0 bar, 25.0°C, and pH 7.0. It is apparent from the graph that both the Na₂SO₄ rejection and water flux of the tested membrane keep nearly constant values of around 94.3% and 87.6 l/m² h, respectively, during the whole testing period, indicating good durability and long-term performance stability.

3.4. Chemical stabilities

Chlorine stability of the obtained composite membrane was evaluated by soaking the membrane samples in a 2000 mg/l sodium hypochlorite aqueous solution for 15.0 h at pH 9.0 and 25.0°C. The salt rejections and water fluxes of the pristine and chlorinated CMCNa/PVA/PSf composite membranes (trial no. 4)

Table 4
Steady-state dye removal and water flux values of the CMCNa/PVA/PSf composite membrane (trial no. 3)

Dye	Molecular weight (g/mol)	Maximum absorbance wavelength (nm)	Steady-state dye removal ^a (%)	Steady-state water flux ^a (l/m ² h)
Methyl blue	799.80	595	99.7	77.3
Congo red	696.7	500	99.5	74.5
Sunset yellow	452.37	480	78.3	80.2

^aTested with 50-mg/l dye aqueous solution at 5.0 bar, 25.0°C, and pH 7.0.

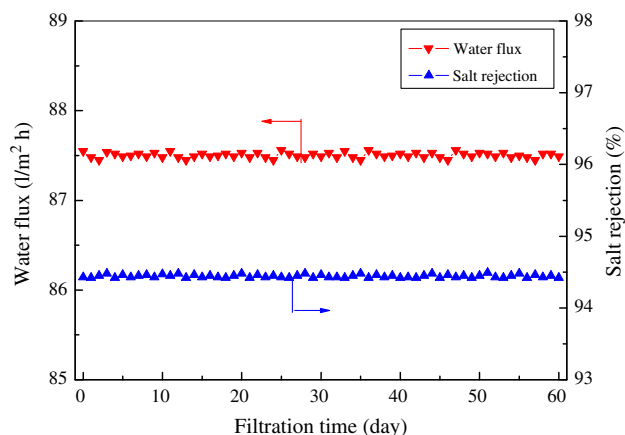


Fig. 9. Changes of water flux (▼) and salt rejection (▲) with filtration time for the CMCNa/PVA/PSf composite membrane (trial no. 5) tested with 500-mg/l Na_2SO_4 aqueous solution at 5.0 bar, pH 7.0, and 25.0°C.

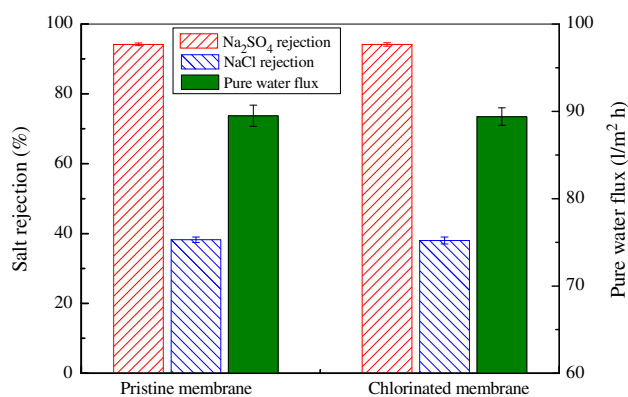


Fig. 10. Pure water fluxes (■) and rejections to Na_2SO_4 (▨) and NaCl (▨) of the pristine and chlorinated CMCNa/PVA/PSf composite membranes (trial no. 4) tested with deionized water and 500-mg/l salt aqueous solution, respectively, at 5.0 bar, pH 7.0, and 25.0°C.

are shown in Fig. 10. It is clear that both the salt rejection and water flux remain nearly constant after chlorination, indicating excellent chlorine stability of the tested membrane.

Table 5

Pure water fluxes and rejections to Na_2SO_4 and NaCl of the pristine, acid-treated, and alkaline-treated CMCNa/PVA/PSf composite membranes (trial no. 4)

Membrane	Pure water flux ^a ($\text{l/m}^2 \text{ h}$)	Rejection to Na_2SO_4 ^b (%)	Rejection to NaCl ^b (%)
Pristine membrane	89.8	94.0	38.2
Acid-treated membrane	90.5	94.1	38.0
Alkaline-treated membrane	89.2	93.8	37.8

^aTested with deionized water at 5.0 bar, pH 7.0, and 25.0°C.

^bTested with 500 mg/l salt aqueous solution at 5.0 bar, pH 7.0, and 25.0°C.

Acid and alkaline resistances of the obtained composite membrane were evaluated by soaking the membrane samples in 0.5 M sulfuric acid and sodium hydroxide aqueous solutions, respectively, for 36.0 h at 25.0°C. The salt rejections and water fluxes of the pristine, acid-treated, and alkaline-treated CMCNa/PVA/PSf membranes (trial no. 4) are presented in Table 5. The very slight changes of salt rejection and water flux after acid or alkaline treatment indicate that the obtained modified membrane possesses good acid and alkaline resistances.

4. Conclusions

In this work, the modification of polysulfone ultrafiltration membrane for NF through sequential deposition of cross-linked PVA and CMCNa has been investigated. The following conclusions can be drawn from the experimental results.

- (1) Negatively charged composite membrane for NF could be obtained through sequential deposition of PVA followed by CMCNa on polysulfone ultrafiltration support membrane with GA cross-linking between each deposition.
- (2) The optimized membrane exhibited a MWCO of about 1,400 Da, a salt rejection order of $\text{MgCl}_2 < \text{NaCl} < \text{MgSO}_4 < \text{Na}_2\text{SO}_4$ at neutral pH, and a good removal performance to the anionic dyes. Under 5.0 bar, the optimized membrane had a high pure water flux of 89.5 $\text{l/m}^2 \text{ h}$ and rejections of 37.8 and 93.8% to 500 mg/l NaCl and Na_2SO_4 aqueous solution, respectively.
- (3) The obtained membrane possessed good durability, performance stability, chlorine stability as well as acid and alkaline resistances. The modification technique developed in this study possesses good repeatability and is potentially applicable for preparing high-flux NF membrane for partial desalination and anionic dye removal.

Acknowledgments

The authors gratefully acknowledge the financial support by the National Natural Science Foundation of China (Grant no. 21476213), the National High-tech R&D Program of China (Grant no. 2012AA03A601), and the 521 personnel training plan of Zhejiang Sci-Tech University.

Funding

NNSFC [Grant Number 21476213].

References

- [1] R.W. Baker, *Membrane Technology and Applications*, second ed., John Wiley & Sons Ltd, Chichester, 2004.
- [2] A.I. Schäfer, A.G. Fane, T.D. Waite, *Nanofiltration-principles and Applications*, Elsevier, New York, NY, 2005.
- [3] P.S. Cartwright, The role of membrane technologies in water reuse applications, *Desalin. Water Treat.* 51 (2013) 4806–4816.
- [4] T. Ahmed, S. Imdad, K. Yaldram, N.M. Butt, A. Pervez, Emerging nanotechnology-based methods for water purification: A review, *Desalin. Water Treat.* 52 (2014) 4089–4101.
- [5] M. Seggiani, M. Puccini, D. Castiello, N. Andreanini, P. Berni, S. Vitolo, Municipal wastewater reclamation and reuse in the leather industry, *Desalin. Water Treat.* 52 (2014) 1647–1653.
- [6] A.M. Hidalgo, G. León, M. Gómez, M.D. Murcia, E. Gómez, P. Penalva, Removal of 4-chloro-2-methylphenol from aqueous solutions by nanofiltration and reverse osmosis, *Desalin. Water Treat.* 53 (2015) 1499–1505.
- [7] B. Barikbin, S.B. Mortazavi, G. Moussavi, Simultaneous removal of Cr(VI) from water containing sulfate using nanofiltration, *Desalin. Water Treat.* 53 (2015) 1895–1901.
- [8] A.W. Mohammad, Y.H. Teow, W.L. Ang, Y.T. Chung, D.L. Oatley-Radcliffe, N. Hilal, Nanofiltration membranes review: Recent advances and future prospects, *Desalination* 356 (2015) 226–254.
- [9] B. Bolto, T. Tran, M. Hoang, Z.L. Xie, Crosslinked poly(vinyl alcohol) membranes, *Prog. Polym. Sci.* 34 (2009) 969–981.
- [10] Y. Liu, R. Wang, H. Ma, B.S. Hsiao, B. Chu, High-flux microfiltration filters based on electrospun polyvinylalcohol nanofibrous membranes, *Polymer* 54 (2013) 548–556.
- [11] H. You, Y. Yang, X. Li, K. Zhang, X. Wang, M. Zhu, B.S. Hsiao, Low pressure high flux thin film nanofibrous composite membranes prepared by electro-spraying technique combined with solution treatment, *J. Membr. Sci.* 394–395 (2012) 241–247.
- [12] D. Bezuidenhout, M.J. Hurndall, R.D. Sanderson, A.J. van Reenen, Reverse osmosis membranes prepared from potassium peroxydisulphate-modified poly(vinyl alcohol), *Desalination* 116 (1998) 35–43.
- [13] T. Zhu, Z. Li, Y. Luo, P. Yu, Pervaporation separation of dimethyl carbonate/methanol azeotrope through cross-linked PVA–poly(vinyl pyrrolidone)/PAN composite membranes, *Desalin. Water Treat.* 51 (2013) 5485–5493.
- [14] F. Peng, Z. Jiang, E.M.V. Hoek, Tuning the molecular structure, separation performance and interfacial properties of poly(vinyl alcohol)-polysulfone interfacial composite membranes, *J. Membr. Sci.* 368 (2011) 26–33.
- [15] G.N.B. Baroña, M. Choi, B. Jung, High permeate flux of PVA/PSf thin film composite nanofiltration membrane with aluminosilicate single-walled nanotubes, *J. Colloid Interface Sci.* 386 (2012) 189–197.
- [16] A.L. Ahmad, N.M. Yusuf, B.S. Ooi, Preparation and modification of poly (vinyl) alcohol membrane: Effect of crosslinking time towards its morphology, *Desalination* 287 (2012) 35–40.
- [17] J.M. Gohil, P. Ray, Polyvinyl alcohol as the barrier layer in thin film composite nanofiltration membranes: Preparation, characterization, and performance evaluation, *J. Colloid Interface Sci.* 338 (2009) 121–127.
- [18] M. Jahanshahi, A. Rahimpour, M. Peyravi, Developing thin film composite poly(piperazine-amide) and poly (vinyl-alcohol) nanofiltration membranes, *Desalination* 257 (2010) 129–136.
- [19] A.D. Shah, C.-H. Huang, J.-H. Kim, Mechanisms of antibiotic removal by nanofiltration membranes: Model development and application, *J. Membr. Sci.* 389 (2012) 234–244.
- [20] M.R. Teixeira, M.J. Rosa, M. Nyström, The role of membrane charge on nanofiltration performance, *J. Membr. Sci.* 265 (2005) 160–166.
- [21] N. Hilal, O.O. Ogunbiyi, N.J. Miles, R. Nigmatullin, Methods employed for control of fouling in mf and uf membranes: A comprehensive review, *Sep. Sci. Technol.* 40 (2005) 1957–2005.
- [22] Y. Ji, Q. An, Q. Zhao, H. Chen, J. Qian, C. Gao, Fabrication and performance of a new type of charged nanofiltration membrane based on polyelectrolyte complex, *J. Membr. Sci.* 357 (2010) 80–89.
- [23] S. Yu, Y. Zheng, Q. Zhou, S. Shuai, Z. Lü, C. Gao, Facile modification of polypropylene hollowfiber microfiltration membranes for nanofiltration, *Desalination* 298 (2012) 49–58.
- [24] S. Rajabzadeh, C. Liu, L. Shi, R. Wang, Preparation of low-pressure water softening hollow fiber membranes by polyelectrolyte deposition with two bilayers, *Desalination* 344 (2014) 64–70.
- [25] C. Liu, L. Shi, R. Wang, Enhanced hollow fiber membrane performance via semi-dynamic layer-by-layer polyelectrolyte inner surface deposition for nanofiltration and forward osmosis applications, *React. Funct. Polym.* 86 (2015) 154–160.
- [26] L.Y. Ng, A.W. Mohammad, C.Y. Ng, C.P. Leo, R. Rohani, Development of nanofiltration membrane with high salt selectivity and performance stability using polyelectrolyte multilayers, *Desalination* 351 (2014) 19–26.
- [27] L.Y. Ng, A.W. Mohammad, C.Y. Ng, A review on nanofiltration membrane fabrication and modification using polyelectrolytes: Effective ways to develop membrane selective barriers and rejection capability, *Adv. Colloid Interface Sci.* 197–198 (2013) 85–107.
- [28] J. Jegal, N.-W. Oh, D.-S. Park, K.-H. Lee, Characteristics of the nanofiltration composite membranes based on PVA and sodium alginate, *J. Appl. Polym. Sci.* 79 (2001) 2471–2479.

- [29] J. Jegal, N.-W. Oh, K.-H. Lee, Preparation and characterization of PVA/SA composite nanofiltration membranes, *J. Appl. Polym. Sci.* 77 (2000) 347–354.
- [30] J. Jegal, K.-H. Lee, Nanofiltration membranes based on poly(vinyl alcohol) and ionic polymers, *J. Appl. Polym. Sci.* 72 (1999) 1755–1762.
- [31] A. Mahmood, S. Bano, S.-G. Kim, K.-H. Lee, Water–methanol separation characteristics of annealed SA/PVA complex membranes, *J. Membr. Sci.* 415–416 (2012) 360–367.
- [32] M. Liu, C. Zhou, B. Dong, Z. Wu, L. Wang, S. Yu, C. Gao, Enhancing the permselectivity of thin-film composite poly(vinyl alcohol) (PVA) nanofiltration membrane by incorporating poly(sodium-p-styrene-sulfonate) (PSSNa), *J. Membr. Sci.* 463 (2014) 173–182.
- [33] S. Bano, A. Mahmood, S.J. Kim, K.-H. Lee, Chlorine resistant binary complexed NaAlg/PVA composite membrane for nanofiltration, *Sep. Purif. Technol.* 137 (2014) 21–27.
- [34] A.E. Childress, M. Elimelech, Effect of solution chemistry on the surface charge of polymeric reverse osmosis and nanofiltration membranes, *J. Membr. Sci.* 119 (1996) 253–268.
- [35] J. Sun, L. Zhang, B. Xie, L. Fan, S. Yu, Separation efficiency and stability of thin-film composite nanofiltration membranes in long-term filtration of copper sulphate and sulphuric acid mixture, *Desalin. Water Treat.* 53 (2015) 1822–1833.
- [36] A.D. Sabde, M.K. Trivedi, V. Ramachandhran, M.S. Hanra, B.M. Misra, Casting and characterization of cellulose acetate butyrate based UF membranes, *Desalination* 114 (1997) 223–232.
- [37] M. Mulder, *Basic Principles of Membrane Technology*, Kluwer Academic Publishers, Boston, MA, 2003.
- [38] P.S. Kalsi, *Spectroscopy of Organic Compounds*, second ed., New Age International Limited Publication, New Delhi, 1996.
- [39] Y. Liu, M. Zhu, Q. Zhao, Q. An, J. Qian, K. Lee, J. Lai, The chemical crosslinking of polyelectrolyte complex colloidal particles and the pervaporation performance of their membranes, *J. Membr. Sci.* 385–386 (2011) 132–140.
- [40] N. Hilal, M. Al-Abri, H. Al-Hinai, M. Abu-Arabi, Characterization and retention of NF membranes using PEG, HS and polyelectrolytes, *Desalination* 221 (2008) 284–293.
- [41] J. Luo, Y. Wan, Effects of pH and salt on nanofiltration—a critical review, *J. Membr. Sci.* 438 (2013) 18–28.
- [42] B. Van der Bruggen, J. Schaep, D. Wilms, C. Vandecasteele, Influence of molecular size, polarity and charge on the retention of organic molecules by nanofiltration, *J. Membr. Sci.* 156 (1999) 29–41.
- [43] W.-J. Lau, A.F. Ismail, Polymeric nanofiltration membranes for textile dye wastewater treatment: Preparation, performance evaluation, transport modeling, and fouling control—A review, *Desalination* 245 (2009) 321–348.